Isı Bilimi ve Tekniği Dergisi, 34, 1, 9-18, 2014
J. of Thermal Science and Technology

ISSN 1300-3615

A SIMPLIFIED THREE-ZONE MODEL FOR DESIGNING SHELL-AND-TUBE REFRIGERANT CONDENSERS

Yusuf Ali KARA
Mechanical Engineering Department, Faculty of Engineering, Ataturk University, 25240 Erzurum, Turkey,
yalikara@atauni.edu.tr

(Geliş Tarihi: 15.05.2012 Kabul Tarihi: 20.09.2012)

Abstract: This paper presents a computer code based on a simplified model for sizing a horizontal shell and tube refrigerant condenser. The model uses three-zone approach for condensing-side and overall approach for the coolant-side of the condenser. Given the thermal and hydraulic data, the code reads many different exchanger configurations from the tube count table and calculates the pressure drop, required heat transfer area and exchanger length for each configuration and then selects the one that has the smallest exchanger area for lowering the initial cost. The model has been experimentally validated by testing a shell-and-tube refrigerant condenser that water flows on tube-side as coolant while R-134a as refrigerant condenses on shell-side. The experimental system is a vapour compression chiller unit using R-134a as refrigerant. The measured and predicted values of the length and the heat transfer area of the tested condenser are in good agreement. The maximum absolute differences between the output of the code and the measured values of the heat rate and heat transfer area are 13% and 7%, respectively.
Keywords: Shell-and-tube refrigerant condenser; condenser design; condenser sizing

GÖVDE -BORU TİPİ ISI DEĞİŞTİRİCİ TASARIMI İÇİN BASİTLEŞTİRİLMİŞ ÜÇ-BÖLGELİ MODEL

Özet: Bu makalede gövde/boru tipi soğutkan yoğuşturucularının boyutlandırılması için basitleştirilmiş bir modele dayanan bir bilgisayar programı sunulmaktadır. Model yoğuşturucunun yoğuşma tarafı için üç-bölgeli, soğutma sıvısı tarafı için tek bölgeli bir yaklaşıma sahiptir. Isıl ve hidrolik verilerin girilmesiyle program, boru yerleştirme tablolarından çok sayıda yoğuşturucu şekline ait geometrik verileri okur, basınç kaybı, gerekli ısı transfer alanı ve ısı değiştiricisi uzunluğunu hesaplayarak maliyeti azaltmak için en küçük ısı transfer alanına sahip olan ısı değiştiricisini belirler. Boru tarafında suyun gövde tarafında ise soğutkan R-134a'nın bulunduğu bir gövde/boru tipi soğutkan yoğuşturucu test edilerek model deneysel olarak doğrulanmıştır. Deney sistemi soğutkan olarak R-134a kullanan buhar sıkıştırmalı bir çiller ünitesidir. Kullanılan yoğuşturucunun gerçek boyutları programın hesapladığı değerlerle karşılaştırılmış ve aralarında iyi bir uyum olduğu belirlenmiştir. Test edilen yoğuşturucunun ısıl gücü ve ısı transfer yüzey alanı için ölçülen ve hesaplanan değerler arasındaki sapma mutlak değerce sırasıyla % 13 ve % 7 olarak belirlenmiştir.
Anahtar Kelimeler: Gövde/boru tipi soğutkan yoğuşturucu, Yoğuşturucu tasarımı, Yoğuşturucu boyutlandırması

NOMENCLATURE

A	Area [m^2]
C	Heat capacity rate [W/K]
c_p	Specific heat [J/kg·K]
D, d	Diameter [m]
F	Correction factor for multi-pass and cross-flow
f	Friction factor
h	Convective heat transfer coefficient [$W/m^2 \cdot K$]
i	Enthalpy [J/kg]
J_c	Segmental baffle window correction factor
J_l	Baffle leakage correction factor
J_b	Bypass correction factor
J_r	Laminar heat transfer correction factor
J_s	Non-equal inlet/outlet baffle spacing correction factor
j_i	Colburn factor
k	Thermal conductivity [W/m·K]
L	Length [m]
$\dot{m}$	Mass flow rate [kg/s]
N	Number
Nu	Nusselt number
P	Pressure [Pa]
PT	Pitch size [m]
Q	Heat rate [W]
Ra	Rayleigh number
R_f	Fouling resistance [$m^2 \cdot K/W$]
T	Temperature [K]
$\overline{T}_c$	Average coolant-side temperature [K]
θ	Temperature difference
S_m	Cross-flow area at the shell centreline within

	one baffle spacing [m^2]
U	Overall heat transfer coefficient [W /m^2 ·K]
u	Velocity [m/s]
x	Quality
μ	Viscosity, [Pa·s]
ρ	Density [kg/m^3]

Subscripts

b	Bulk
c	Cold, coolant
cd	Condenser
cf	Counter flow
eff	Effective
est	Estimated
ex	Exchanger
ev	Evaporator
f	Fouling
fg	Latent
g,go	Vapour, gas only
h	Hot
i	Inlet, inner, in
id	Ideal
J	Number of zone
L, l	Liquid
lm,lo	Logarithmic mean, liquid only
m	Mean
N	Nusselt
o	Outer, out
p	Pass
r	Refrigerant
s	Shell
sat	Saturation
sb	Sub-cooling
sh	Superheat
t	Tube
tot	Total
tp	Two-phase
w	Wall

Superscripts

n	exponent

INTRODUCTION

Horizontal shell-side condensers, which are the objective of this study, are widely used in vapour-compression air-conditioning and refrigeration applications. In such a condenser, the refrigerant vapour enters the shell in a superheated condition. It is cooled to the saturation temperature and then completely condensed by the coolant, which is usually water flowing through the inside of horizontal tubes. The liquid condensate may be sub-cooled to a temperature that is lower than the saturation temperature. Typical designs have one pass on shell-side with an E-shell, and two or four passes on the tube-side.

Sizing of a heat exchanger is known to be a design problem. Webb and Robertson (1988) provided the mechanical design features of horizontal shell-side refrigerant condenser. Mohanty (1988) presented a computer code for designing horizontal shell-side steam condensers. His conservative model is based on the Logarithmic Mean Temperature Difference (LMTD) method and ignores both de-superheating and sub-cooling zones. It is assumed that steam enters the condenser at the saturation temperature. Rubin (1981) contributed some new terms such as wet de-superheating zone and dry de-superheating zone to make the heat transfer phenomena in a de-superheating zone more readily understood. He emphasised that if the inlet end of the condenser is so designed that the superheated vapour has no access to a condensate, the presence of a dry de-superheating zone should be considered in the design calculations because the superheat in a vapour is removed by convective heat transfer across the tube wall in the dry de-superheating zone, while it is removed by a condensing mechanism in the wet de-superheating zone, where superheated vapour is in direct contact with a condensate. Burlingame (1984) has presented an incremental design model using the weighted Mean Temperature Difference (MTD) method to design a shell and tube condenser with multicomponent vapour condensing or single vapour condensing in the presence of a non-condensing gas on the shell side. The weighted MTD equals the total heat exchanged divided by the summation of the heat exchanged per zone divided by the LMTD per zone. The overall heat transfer coefficient is determined by dividing the total heat exchanged by the product of the total surface and the weighted MTD. In multicomponent condensation, the effect of the gas phase resistance to heat transfer is usually accounted for using the method published by Bell and Ghaly (1973). An incremental procedure is suggested by Webb and Panagoulias (1987) to design a multi-component shell and tube condenser by employing the film theory method. In the film theory method, concentration and temperature differences between the bulk vapour and the vapour-liquid interface are assumed to occur across a thin laminar film adjacent to the interface.

Ferrari at al. (1986) presented a computer code based on the finite differences method for designing a full plate baffled shell-and-tube condenser with condensing in the presence of a non-condensing gas on the shell-side. Hewitt et al. (1994) gave governing equations for the design problem of a shell-side condenser. He employed the LMTD method in his multi-zone condenser model. Conversely, tube wall temperature is not inserted into his model, which is needed to calculate the heat transfer coefficients. Mueller (2002) introduced Butterworth's stepwise calculation procedure. In Butterworth's design method, first of all, temperature-enthalpy curves for two

fluid streams are plotted using an iterative procedure that is independent of heat transfer coefficients and the detailed geometry of the exchanger. Next, the heat transfer calculations are made for various selected geometries to establish the exchanger area and length. However, Butterworth's design method is valid only for E-type shell with two tube-side passes. Mueller (2002) also introduced Emerson's design method that can be used for an infinite number of tube passes. Temperature of the coolant assumed to be constant throughout the exchanger in Emerson's method. Another stepwise calculation suggested by Bell and Mueller is also given in (Mueller, 2002). The procedure is appropriate for only two passes of the coolant and based on determining the fraction of tubes to be flooded. These methods are also used for multi-component condensers. Paul (1986) presents the stochastic geometric model to design a horizontal shell and tube condenser for industrial refrigeration plants. Marto (1984) gives a review for computer modelling of the shell and tube condenser design with the presence of incondensable gases. There are numerous papers in (Butterworth, 1983) related to the design of power or process condensers that involve multi-component condensation. Condensation curves of pure vapour condensation and multi-component condensation are different. Conversely, horizontal shell-side refrigerant condensers involve pure vapour condensation. García et al. (2010) provides a model that can be used with heat exchangers when they are working as refrigerant condensers or evaporators. Llopis et al. (2008) presents a dynamic model of a shell-and-tube refrigerant condenser operating in a vapour compression refrigerant plant. The model is based on mass continuity, energy conversation and heat transfer physical fundamentals. Karlsson and Vamlin (2005) carried out 2D calculations to determine the vapour flow field and condensation rate of a shell-and-tube refrigerant condenser.

This paper presents a design code based on a simplified model using the three-zone approach for the study of water-cooled shell-and-tube refrigerant condensers. Given the thermal and hydraulic data, i.e. T_{sat}, $T_{r,i}$, $T_{r,o}$, $T_{c,i}$, $\dot{m}_r$, $\dot{m}_c$, the code calculates the exit temperature of the coolant from the energy balance of the condenser. After reading the shell diameter, tube diameter, tube number and pitch size from the tube count table, the code evaluates the necessary heat transfer coefficients to determine the required heat transfer area and length of the condenser and finally calculates the pressure drops on both sides. The code examines numerous exchangers by varying the exchanger configuration from tube count and selects the one that has the smallest exchanger area to reduce the initial cost. Although heat exchanger designers already have their own in-company design codes, the author believes that this code could be of interest to practicing heat exchanger engineers or researchers who want to make a computer simulation of any thermal system that has a refrigerant condenser. The code can be easily employed as a subroutine to a thermal system simulation code for preliminary design purposes. Despite its simplicity, the model proves to be useful to the pre-design and correct selection of shell-and-tube condensers working at full and complex refrigeration systems.

MODEL DESCRIPTION

The model is based on the three-zone modelling approach as shown in Figure-1. In the de-superheating zone, refrigerant vapour enters the condenser in a superheated condition at temperature $T_{r,i}$ and cools to temperature $T_{r,sh}$ where the tube wall temperature reaches the dew point temperature and condensation just commences on the surface and the coolant temperature is $T_{c,sh}$ at this point. This is actually called the dry wall de-superheating zone, in which some of the sensible heat of superheated vapour is transferred across the tube wall to the coolant.

After this point, the superheated vapour is in direct contact with the condensate and cooled to saturation temperature $T_{sat,}$ while condensation simultaneously occurs on the tube surface. This region is called the wet wall de-superheating zone and the entire vapour is at the saturation temperature at the end of this zone. After that, the condensation continues at the saturation temperature until the entire vapour disappears and the coolant temperature reaches $T_{c,tp}$ at the end of the condensing zone. The liquid condensate in the sub-cooling zone may then be sub-cooled to a temperature that is lower than the saturation temperature. In the present model, the wet wall de-superheating zone is lumped into the condensing zone and constant wall temperature is assumed in each zone. Heat loss from the condenser outer surface to the ambient is ignored.

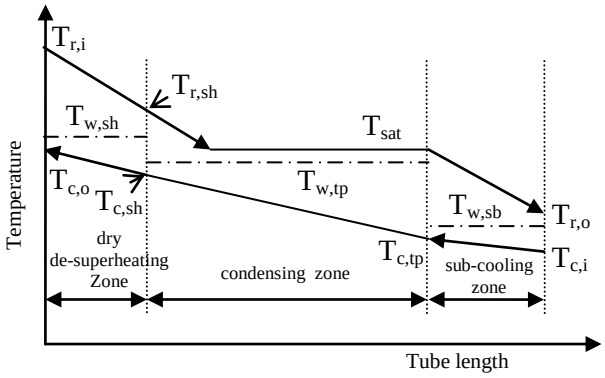

Figure 1. Temperature distribution in the condenser

Logarithmic mean temperature difference for pure counter-flow:

$$\Delta T_{lm,cf} = \frac{\Delta T_1 - \Delta T_2}{ln\left(\frac{\Delta T_1}{\Delta T_2}\right)} \quad (1)$$

Where

$$\Delta T_1 = T_{h,i} - T_{c,o} \; ; \; \Delta T_2 = T_{h,o} - T_{c,i} \quad (2)$$

The effective mean temperature difference for cross-flow:

$$\Delta T_m = F \Delta T_{lm,cf} \quad (3)$$

where F is correction factor for multi-pass and cross-flow heat exchanger and given as follows;

$$F = \frac{\left(\sqrt{R^2+1}\right) ln\left[\frac{1-P}{1-PR}\right]}{(R-1) ln\left[\left(2-P\left(R+1-\sqrt{R^2+1}\right)\right)/\left(2-P\left(R+1+\sqrt{R^2+1}\right)\right)\right]} \quad (4)$$

where,

$$R = \frac{C_c}{C_h} = \frac{T_{h,i}-T_{h,o}}{T_{c,o}-T_{c,i}} \quad (5)$$

and

$$P = \frac{T_{c,o}-T_{c,i}}{T_{h,i}-T_{c,i}} \quad (6)$$

Overall heat transfer coefficient:

$$U = \frac{1}{\frac{d_{t,o}}{d_{t,i}h_t}+\frac{d_{t,o}R_{f,i}}{d_{t,i}}+\frac{d_{t,o}\ln\left(\frac{d_{t,o}}{d_{t,i}}\right)}{2k_{cd}}+R_{f,o}+\frac{1}{h_s}} \quad (7)$$

The model is introduced in a computer execution manner to make it easy to understand.

Sub-cooling zone

Known variables: $T_{r,o}$, T_{sat} , $T_{c,i}$, $\dot{m}_c$, $\dot{m}_r$
Unknown variables: Q_{sb} , $T_{c,tp}$, A_{sb}, $T_{w,sb}$
Calculate $i_{r,i}$ at (P_{sat} ,$T_{r,i}$), $i_{r,o}$ at (P_{sat} ,$T_{r,o}$), and $c_{p,c}$ at $T_{c,i}$

$$T_{c,o} = \frac{\dot{m}_r(i_{r,i}-i_{r,o})}{\dot{m}_c c_{p,c}} + T_{c,i} \quad (8)$$

$$C_{c,sb} = \dot{m}_c * c_{p,c} \quad (9)$$

$$T_{r,m,sb} = (T_{r,o}+T_{sat})/2 \quad (10)$$

Evaluate $c_{p,r,sb}$ at $T_{r,m,sb}$

$$C_{r,sb} = \dot{m}_r * c_{p,r,sb} \quad (11)$$

$$Q_{sb} = C_{r,sb} * (T_{sat} - T_{r,o}) \quad (12)$$

$$T_{c,tp} = Q_{sb}/C_{c,sb}+T_{c,I} \quad (13)$$

$$T_{c,m,sb} = (T_{c,tp} + T_{c,i})/2 \quad (14)$$

Re-evaluate $c_{p,c}$ at $T_{c,m,sb}$ and go to 5 and recalculate Eqs. (9-13)
Evaluate $h_{c,sb}$ using Eqs. (38-40)

$$T_{w,sb,est} = (T_{r,m,sb} + T_{c,m,sb})/2 \quad (15)$$

Evaluate $h_{r,sb}$ from Eq.(43) by inserting $T_{w,sb,est}$ get U_{sb} and $\Delta T_{lm,sb}$ from Eqs. (1-7)

$$A_{sb} = Q_{sb}/(U_{sb} * \Delta T_{lm,sb}) \quad (16)$$

$$T_{w,sb} = T_{r,m,sb} - Q_{sb}/(A_{sb} * h_{r,sb}) \quad (17)$$

Re-evaluate $h_{r,sb}$ by using $T_{w,sb}$ and go to 10 and recalculate Eqs. (16-17)

Transport properties of both fluids are evaluated at mean temperatures. $\Delta T_{lm,sb}$ and U_{sb} are calculated from Eqs. (1-7) by replacing $T_{h,i}$,$T_{h,o}$,$T_{c,o}$, h_t , h_s with T_{sat}, $T_{r,o}$, $T_{c,tp}$, $h_{c,sb}$ and $h_{r,sb}$, respectively.

Condensing zone

Known variables: T_{sat}, $T_{c,tp}$, $\dot{m}_c$, $\dot{m}_r$
Unknown variables: $T_{r,sh}$, $T_{c,sh}$, $T_{w,tp}$, A_{tp}, Q_{tp}
Guess initial values of the $T_{r,sh}$, $T_{c,sh}$, $T_{w,tp}$, A_{tp}

$$T_{c,m,tp} = (T_{c,sh} + T_{c,tp})/2$$

Evaluate $h_{c,tp}$ from Eqs. (38-40) and $h_{r,tp}$ from Eqs. (33-38), calculate $c_{p,r,sh}$, U_{tp}, $\Delta T_{lm,tp}$

$$C_{c,tp}\,(T_{c,sh} - T_{c,tp}) - \dot{m}_r\,[c_{p,r,sh}\,(T_{r,sh} - T_{sat}) + i_{fg}] = 0 \quad (18)$$

$$A_{tp}\,U_{tp}\,\Delta T_{lm,tp} - \dot{m}_r\,[c_{p,r,sh}\,(T_{r,sh} - T_{sat}) + i_{fg}] = 0 \quad (19)$$

$$A_{tp} h_{r,tp}(T_{sat} - T_{w,tp}) - \dot{m}_r\,[c_{p,r,sh}(T_{r,sh} - T_{sat}) + i_{fg}] = 0 \quad (20)$$

$$A_{tp}\,h_{c,tp}\,(T_{w,tp} - T_{c,m,tp}) - \dot{m}_r\,[c_{p,r,sh}\,(T_{r,sh} - T_{sat}) + i_{fg}] = 0 \quad (21)$$

The set of Eqs. (18-21) is solved by employing the Newton-Raphson method and then the heat transfer rate in the condensing zone can be calculated as follows,

$$Q_{tp} = \dot{m}_r\,[c_{p,r,sh}\,(T_{r,sh} - T_{sat}) + i_{fg}] \quad (22)$$

The first term of Eq. (22) considers wet wall de-superheating. The transport properties of both fluids are evaluated at mean temperatures. $\Delta T_{lm,tp}$ and U_{tp} are calculated from Eqs. (1-7) by replacing $T_{h,i}$, $T_{h,o}$, $T_{c,i}$, $T_{c,o}$, h_t, h_s with $T_{r,sh}$, T_{sat}, $T_{c,tp}$, $T_{c,sh}$, $h_{c,tp}$, $h_{r,tp}$, respectively.

De-superheating zone

Known variables: $T_{r,sh}$, $T_{c,sh}$, $T_{r,i}$, $T_{c,o}$, $\dot{m}_c$, $\dot{m}_r$
Unknown variables: A_{sh} , Q_{sh} , $T_{w,sh}$

$$T_{r,m,sh} = (T_{r,i}+T_{r,sh})/2 \quad (23)$$

Get $c_{p,r,sh}$ at $T_{r,m,sh}$

$$C_{r,sh} = \dot{m}_r\ c_{p,r,sh} \quad (24)$$

$$Q_{sh} = C_{r,sh}\,(T_{r,i} - T_{r,sh}) \quad (25)$$

$$T_{c,m,sh} = (T_{c,o} + T_{c,sh})/2 \quad (26)$$

Evaluate $h_{c,sh}$ from Eqs. (38-40)

$$T_{w,sh,est} = (T_{r,m,sh} + T_{c,m,sh})/2 \quad (27)$$

Evaluate $\mu_{r,sh}$ at $T_{w,sh,est}$ and calculate $h_{r,sh}$ from Eqs. (41-42)
Get U_{sh} and $\Delta T_{lm,sh}$

$$A_{sh} = Q_{sh}/(U_{sh} * \Delta T_{lm,sh}) \quad (28)$$

$$T_{w,sh} = T_{r,m,sh} - Q_{sh}/(A_{sh} * h_{r,sh}) \quad (29)$$

Re-evaluate $h_{r,sh}$ at $T_{w,sh}$ and go to 20 and recalculate Eqs. (28-29)

The transport properties of both fluids are evaluated at mean temperatures. $\Delta T_{lm,tp}$ and U_{tp} are calculated from Eqs. (1-7) by replacing $T_{h,i}$, $T_{h,o}$, $T_{c,i}$, h_t, h_s with $T_{r,i}$, $T_{r,sh}$, $T_{c,sh}$, $h_{c,sh}$, $h_{r,sh}$ respectively. The total condenser area, condenser length, and total heat rate are calculated as follows,

$$A_{tot} = A_{sb} + A_{tp} + A_{sh} \quad (30)$$

$$L_{ex} = A_{tot}/(\pi\, N_t\, d_{t,o}) \quad (31)$$

$$Q_{tot} = Q_{sb} + Q_{tp} + Q_{sh} \quad (32)$$

CONDENSATION HEAT TRANSFER COEFFICIENT

There are several published studies on the prediction of the heat transfer coefficient during shell-side condensation in open literature. Marto (1984) has reviewed the shell-side condensation and pressure drop. The most recent review on this issue is published by Brown and Baysal (1999). Shell-side condensation heat transfer coefficient is mainly affected by tube surface geometry, vapour velocity and condensate inundation. Because it considers the combined effect of both vapour shear and inundation, the Butterworth correlation as given in (Marto, 1984) is used in the present paper. The combined average heat transfer coefficient for shell-side

condensation with *n* plain tube in a vertical row can be predicted as follows,

$$h_{tp} = n^{-0.16}\left[\frac{1}{2}h_{sh}^2 + \left(\frac{1}{4}h_{sh}^4 + h_N^2\right)^{0.5}\right]^{0.5} \quad (33)$$

where

$$h_{sh} = 0.594\,\frac{k_L}{d_{t,o}}Re_{tp}^{0.5} \quad (34)$$

where Re_{tp} is two-phase Reynolds number defined as follows,

$$Re_{tp} = \frac{u_g \rho_L d_{t,o}}{\mu_L} \quad (35)$$

h_N in Eq. (33) is the well-known Nusselt equation for condensation on a single horizontal tube,

$$h_N = 0.728\left[\frac{g k_L^3 \rho_L(\rho_L - \rho_g) i_{fg}}{d_{t,o}\mu_L(T_{sat} - T_{w,tp})}\right]^{0.25} \quad (36)$$

Because superheated vapour enters the condenser, according to Webb's recommendation (Webb, 1984), the latent heat i_{fg} in Eq. (36) is replaced with i'_{fg} given by Eq. (37) to account for the effect of vapour superheat.

$$i'_{fg} = i_{fg} + c_{p,r,sh}\left(T_{r,sh} - T_{sat}\right) \quad (37)$$

SINGLE PHASE HEAT TRANSFER COEFFICIENTS

Kakaç (1998) gives a detailed review for the tube-side heat transfer coefficient for both laminar and forced convection flow conditions. Considering his recommendations, Schlünder, Gnielinski and Petukov-Kirillov correlations are employed for laminar, transition and turbulent flow, respectively in order to calculate the tube-side heat transfer coefficient. The single phase heat transfer coefficient on the shell-side for the superheated zone is evaluated using the model given by Taborek (2002) based on the Bell-Delaware method. Single segmental baffles with vertical cut that cause the vapour to flow side-to-side are commonly used on the shell-side. The lower edges of the baffles are notched to permit draining. According to Webb (1984), baffles may not be used in refrigerant condensers to minimise pressure loss. In this case, in addition to the baffled shell, the single phase heat transfer coefficient for un-baffled shell can also be calculated simply by taking the combined effect of all correction factors as unity in the Bell correlation, i.e. J_{tot} = 1 in Eq. (41) and this is a significant advantage of the Bell correlation for the computer code. According to Rubin (1981), there are three mechanisms of sub-cooling. The film-type sub-cooling occurs when an excess surface area exists, submerged sub-cooling with natural or forced convection occurs when a liquid level is maintained in the shell. Submerged sub-cooling is attained by using a dam type baffle near the condensate outlet to create a pool partially submerging the bundle. A condenser with submerged sub-cooling may be preferred in small-sized refrigerating plants since it can also serve as a liquid receiver. As a consequence, submerged sub-cooling with natural convection is assumed in the present paper, and heat transfer coefficient for the sub-cooled region is evaluated by employing Churchill and Chu correlation (Incropera et al., 2007). The correlations referred in this section are listed below for the reader convenience;
Schlünder correlation for laminar flow;

$$\boldsymbol{Nu} = \left[\mathbf{3.66^3} + \mathbf{1.61^3}\left(\frac{\boldsymbol{Pe_b d_{t,i}}}{\boldsymbol{L_t}}\right)\right]^{\mathbf{1/3}} \quad (38)$$

Gnielinski correlation for transition flow in the range of 2300 <Re<10^4

$$\boldsymbol{Nu} = \frac{(f/2)(\boldsymbol{Re_b} - \mathbf{1000})\boldsymbol{Pr_b}}{\mathbf{1+12.7}(f/2)^{1/2}\left(\boldsymbol{Pr_b^{2/3}} - \mathbf{1}\right)} \quad (39)$$

Petukov-Kirillov correlation for turbulent flow in the range of 10^4 <Re< 5x10^6

$$\boldsymbol{Nu} = \frac{(f/2)\boldsymbol{Re_b Pr_b}}{\mathbf{1.07+12.7}(f/2)^{1/2}\left(\boldsymbol{Pr_b^{2/3}} - \mathbf{1}\right)} \quad (40)$$

where,

$$\boldsymbol{f} = (\mathbf{1.58}\boldsymbol{lnRe_b} - \mathbf{3.28})^{-2}$$

Bell correlation;

$$\boldsymbol{h_s} = \boldsymbol{h_{id}}(\boldsymbol{J_c})(\boldsymbol{J_l})(\boldsymbol{J_b})(\boldsymbol{J_r})(\boldsymbol{J_s}) = \boldsymbol{h_{id}}(\boldsymbol{J_{tot}}) \quad (41)$$

$$\boldsymbol{h_{id}} = \boldsymbol{j_i c_{p,s}}\left(\frac{\dot{\boldsymbol{m}}_{\boldsymbol{s}}}{\boldsymbol{S_m}}\right)(\boldsymbol{Pr_s})^{-2/3}\left(\frac{\boldsymbol{\mu_{s,b}}}{\boldsymbol{\mu_{s,w}}}\right) \quad (42)$$

The correlations for correction factors in Eq. (41) and for j_i - Colburn factor in Eq. (42) are available in (Taborek, 2002). Churchill and Chu correlation 10^{-5} < Ra < 10^{12};

$$\boldsymbol{Nu} = \left\{\mathbf{0.6} + \frac{\mathbf{0.387}\boldsymbol{Ra}^{\mathbf{1/6}}}{\left[\mathbf{1+(0.559/}\boldsymbol{Pr}\mathbf{)^{9/16}}\right]^{\mathbf{8/27}}}\right\}^{\mathbf{2}} \quad (43)$$

PRESSURE DROP CORRELATIONS

The correlation given by Grant and Chisholm (1979) is used for the prediction of the two-phase flow pressure drop in shell. Their method makes it possible to calculate the pressure drop in a cross-flow section and window section separately.

$$\psi = \frac{\frac{\Delta P_{tp}}{\Delta P_{lo}} - 1}{\Gamma^2 - 1} \quad (44)$$

where ΔP_{tp} is two-phase flow pressure drop and Γ is physical property coefficient defined by,

$$\Gamma = \left(\frac{\Delta P_{go}}{\Delta P_{lo}}\right)^{1/2} \quad (45)$$

where ΔP_{go} and ΔP_{lo} are the pressure drops for the total mass flowing as gas and liquid, respectively. For horizontal side-to-side flow in cross-flow zone of tube bundle, the correlation for the parameter Ψ in Eq. (44) is given as follows,

$$\psi = Bx^{(2-n)/2}(1-x)^{(2-n)/2} + x^{2-n} \quad (46)$$

where B is 0.75 for spray and bubbly flow or 0.25 for stratified and stratified-spray flow, n is 0.46 for both cases, and x is the vapour quality. The correlation for the window zone is as follows,

$$\psi = Bx(1-x) + x^2 \quad (47)$$

where

$$B = \frac{2}{\Gamma^2+1} \quad (48)$$

In order to predict ΔP_{go} and ΔP_{lo} in Eqs. (44- 45), Taborek correlation (2002) is used since it also makes it possible to calculate single phase flow pressure drops in the cross-flow section and window section separately. Kakaç (1998) recommends the following equations for tube-side pressure drop,

$$\Delta P_t = \frac{\rho u_m^2}{2}\left(4f\frac{L_{ex}N_p}{d_{t,i}} + 4N_p\right) \quad (49)$$

where f is the friction factor and it can be calculated in the range of $3 \times 10^4 < Re < 10^6$ as follows,

$$f = 0.046\ Re^{-0.2} \quad (50)$$

The second term in Eq. (49) is due to the change of direction in the tube passes.

THERMODYNAMIC PROPERTIES

Certain thermodynamic and transport properties of R-134a and water are needed for the model. There are several published works reporting the thermodynamic properties of R-134a in open literature. The equations given by Cleland (1994) are used to evaluate the enthalpy, saturation pressure and saturation temperature, since these equations are very simple and easy to use. The specific volume, constant pressure specific heat and constant volume specific heat of the superheated vapour of R-134a are calculated using Stegou's equations (Stegou, 1997) . The liquid density of the refrigerant is calculated from the equation given by Basu and Wilson (1989). The thermal expansion coefficient of liquid R-134a can be obtained from the equation given in (Shunk, 2002), although the effect of pressure varying with temperature is neglected in this equation. Therefore, the equation given by Incropera et al. (2007) is employed in the present paper. The saturated thermophysical properties of both liquid and vapour of R-134a such as viscosity and thermal conductivity, and constant pressure specific heat of saturated liquid of R-134a and the thermophysical properties of saturated water such as viscosity, thermal conductivity, density, and specific heat are evaluated by interpolating the data given in ASHRAE and the water tables. For interpolating data the Newton- Gregory interpolation method is employed.

SOLUTION LOGIC FOR THE MODEL

A design code can be established in any computer programming environment such as FORTRAN or MATLAB to solve the model. The flow chart of the code is shown in Figure-2. The design code starts inputting thermal and hydraulic data and then reads the number of tubes by altering the shell diameter, pass number and tube diameter and pitch size respectively from the tube counts (Saunders, 2002). The heat transfer area, exchanger length, and pressure drops are calculated for every configuration. After analysing all of the exchangers according to the model, the code selects the one that has the smallest value for the heat transfer area.

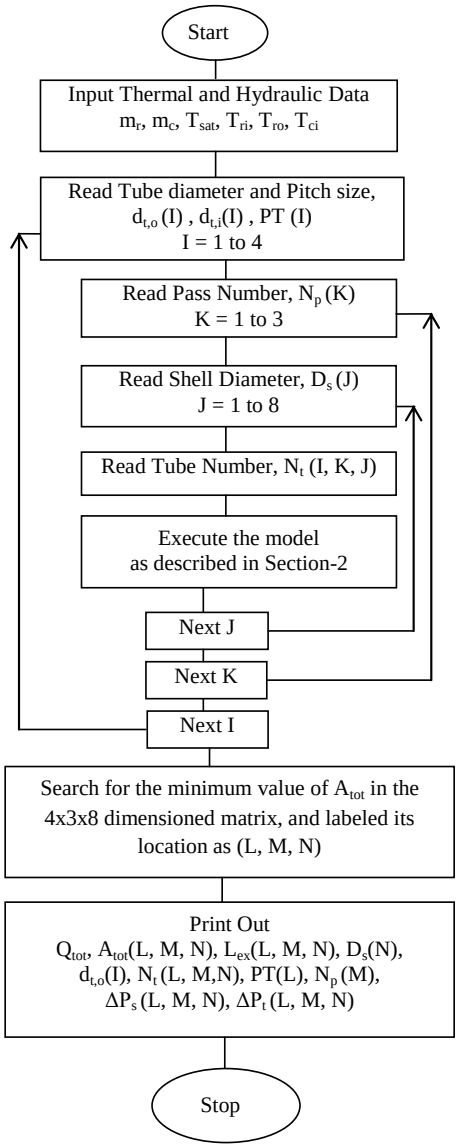

Figure 2. Flowchart of design code

MODEL VALIDATION

A small sized chiller system was set up to validate the model. The system consisted of a water heater as the heat source, a compressor, condenser, evaporator, thermostatic expansion valve, liquid tank, i.e., receiver, and fan-coil units that remove the heat from the condenser. The water heater (8) was equipped with an electrical heater that was controlled by a digital thermostat in order to ensure the desired water temperature as a heat source to the evaporator. Refrigerant 134a was used as the working fluid. The vapour compression chiller had an electrically-driven Copeland scroll compressor (1) working with R-134a. The condenser (2) was a fixed tube sheet shell and tube exchanger that has four tube passes with plain tubes, one shell pass, and R-134a condensed on shell-side, while water as a coolant flowed in tubes. The evaporator

(6) was also shell and tube type exchanger having one shell pass and two tube-passes. Water flowed in the shell, while R-134a boiled in plain tubes in the evaporator. A thermostatic expansion valve was used for the throttling process. The illustration of the experimental system is shown in Figure 3. A Krohne electromagnetic flow meter (4) was placed on the liquid line of R-134a after the receiver to measure the refrigerant flow rate. The flow meter indicator was calibrated for R-134a by its manufacturer with the accuracy of ±8% of full scale. Although the fluctuations of the refrigerant flow were too low with the scroll-type compressor, a receiver was used before the flow meter to ensure the flow stability. Water flow rates were measured by using the Cole-Parmer spring loaded variable area type flow meters (7) that had a direct reading scale and cylindrical float. The accuracy of the water flow meters is ±7% of full scale.

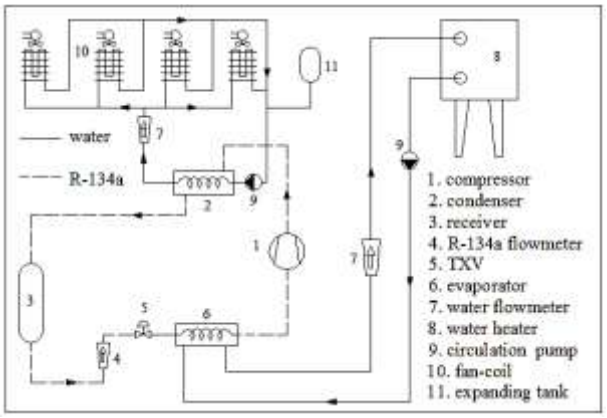

Figure-3. The experimental set up

The condensation and evaporation pressures were measured with Cole-Parmer pressure transmitters with an accuracy of ±1% of full scale, and temperatures were measured using a Cole-Parmer PVC insulated thermocouple probes with a PVC-coated tip that ensures electrically isolation. Thermocouples were calibrated in the range of 20-90˚C using a standard water bath and the accuracy was ±0.4˚C. Temperatures and pressures were monitored and stored with Advantech DAQ card.

The experimental study was carried out at different working conditions, namely Case-1 through Case-7. In order to change the working conditions, the condensing pressure was changed by employing 2, 3 and 4 fan-coils in each case from Case-1 to Case-3; conversely, evaporation pressure was changed by adjusting the thermostatic expansion valve in each case from Case-4 to Case-7. In each case, the experimental data was recorded after reaching steady state conditions. The measured data is shown in Table-1. The saturation temperature corresponding to the measured saturation pressure was calculated and inserted into Table-1 for the reader's convenience. An uncertainty analysis was carried out using the Kline and McClintock method as it is given by Holman (1994), and the heat rate calculation could be in error up to 11%.

In addition to the experimental validation, a computer program was written based on Emerson's method, which is a well-known model in the literature, and the results of the current design program and Emerson's method were compared to demonstrate that the current design program yields true results. Temperature of the coolant assumed to be constant throughout the exchanger in Emerson's method and (Mueller, 2002). Emerson's method was briefly given in Appendix-A for the reader convenience.

Table 1 Experimentally measured data

Parameters	Unit	Case-1	Case-2	Case-3	Case-4	Case-5	Case-6	Case-7	Uncertainty
$\dot{m}_r$	(LPH)[a]	80	80	80	65	75	90	90	±8%
$\dot{m}_w$	(LPM)[a]	10	10	10	10	10	11	10	±7%
$T_{w,i}$	(°C)	56.4	51.2	46.1	50.7	46.7	53.0	58.6	±0.4°C
$T_{w,o}$	(°C)	61.4	56.4	51.6	55.1	51.9	58.1	64.0	±0.4°C
$T_{r,i}$	(°C)	82.3	77.2	70.0	76.9	73.5	74.7	83.4	±0.4°C
$T_{r,o}$	(°C)	60.2	55.8	51.3	54.4	51.9	56.8	62.6	±0.4°C
P_{cd}	(bar)	18	16	14	15.5	14.2	16.5	19	±1%
P_{ev}	(bar)	4	4	4	3.4	3.8	4.2	4.5	±1%
T^b_{sat}	(°C)	62.9	57.9	52,4	56.6	52.9	59.2	65.2	±1%
Q^b_{tot}	(W)	3,405	3,572	3,734	3,027	3,558	3,814	3,708	±11%

[a] measured raw data, LPH = Litre Per Hour, LPM = Litre Per Minute
[b] saturation temperature corresponding to the P_{cd}, calculated
[c] calculated from the coolant side

RESULTS AND DISCUSSION

Because the dimensions of the tested condenser are not included in the tube counts, apart from the design code, a validation code is written executing the same mathematical model as the design code. In other words, there are two codes; one is the validation code and the other is the design code. The validation code is derived from the design code. Both of the codes use the same model. The only difference between the validation and the design codes is that the former executes the model for only one condenser, i.e. tested condenser to determine its heat transfer area and length, the latter does the same job for several condensers and chooses the one that has the smallest heat transfer area.

When the working conditions given in the Table-1 and the geometrical dimensions of the tested condenser are input, the validation code solves the model given in Section-2 to determine the heat transfer area and the length of the tested condenser. The algorithm of this code is given in Figure-4. The validation code can also be used to determine the area and length of any condenser that its configuration is out of standard. However, the user should input the configuration of the condenser to the validation code.

The results from the validation code for the tested condenser are given in Table-2. The tested condenser consisted of a typical 1-pass-E-shell and a 4-pass-tube bundle as shown in Figure-5. The results of the validation code are in good agreement with the actual parameters. The maximum absolute differences between the output of the code and the measured values of the heat rate and heat transfer area are 13% and 7%, respectively.

Table 2. Results for experimental validation

Parameters	Case-1	Case-2	Case-3	Case-4	Case-5	Case-6	Case-7	Tested condenser	Maximum deviation
Q^*_{tot} (W)	3,837	4,027	3,972	3,347	3,958	4,203	4,162		12.7%
A_{tot} (m^2)	1.0462	1.0426	1.059	0.9958	1.0958	1.0943	1.1078	1.0314	7.3%
L_{ex} (m)	0.771	0.768	0.78	0.734	0.807	0.806	0.816	0.76	7.3%

* calculated from the refrigerant side

These are acceptable errors considering the uncertainty of the heat load, which is 11%.

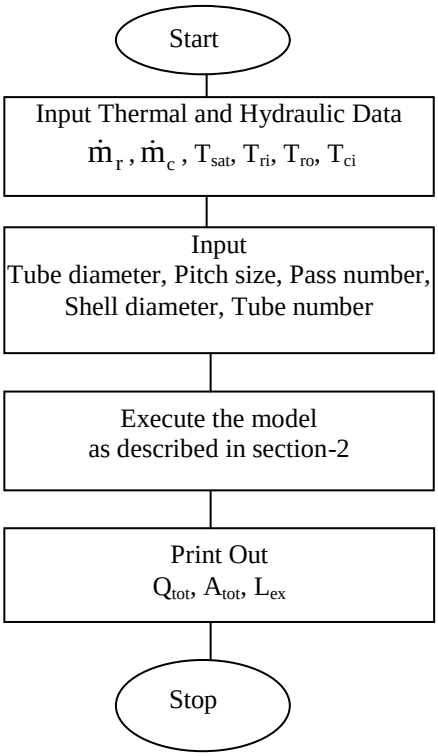

Figure 4. Flowchart of the validation code

The design code selects the condenser with the smallest surface area among a total number of 96 exchangers included in the tube counts. It also calculates the pressure drops of both streams. It is restricted to the exchanger configuration of the fixed tube sheet, one-shell-pass, and one, two, and four-tube passes and triangular pitch. The shell diameter range is limited from 203mm up to 540mm. The tube outer diameters are 15.88mm, 19.05mm, 25.4mm, 31.75mm and pitch sizes are 19.84mm, 23.81mm, 31.75mm and 39.69mm. The code can be extended to cover more configurations and dimensions simply by inserting more tube count data.

The results of the design code are given in Table-3. By ignoring the small differences in the area of selected exchangers it can be readily seen from Table-3 that the design code selects the same condenser for the each working condition. It means that each working condition given in Table-1 can be satisfied with the same condenser. This is an expected result considering that given working conditions are measured using the one tested condenser.

Table 3. Results of thedesign code

Parameters	Case-1	Case-2	Case-3	Case-4	Case-5	Case-6	Case-7
Q^*_{tot}(W)	3,842	4,031	3,975	3,351	3,961	4,371	4,168
A_{tot} (m^2)	1.0977	1.0884	1.0941	1.0565	1.1561	1.1774	1.1522
L_{ex} (m)	0.489	0.485	0.487	0.471	0.515	0.524	0.513
D_s (m)	0.203	0.203	0.203	0.203	0.203	0.203	0.203
d_{to} (m)	0.01588	0.01588	0.01588	0.01588	0.01588	0.01588	0.01588
PT (m)	0.01984	0.01984	0.01984	0.01984	0.01984	0.01984	0.01984
N_t	45	45	45	45	45	45	45
N_p	4	4	4	4	4	4	4
ΔP_s (Pa)	13.9	18.9	18.7	29.7	7.4	6.8	7.4
ΔP_t (Pa)	14.1	14.1	14.1	14.3	14.5	17.4	14.3

* calculated from the refrigerant side

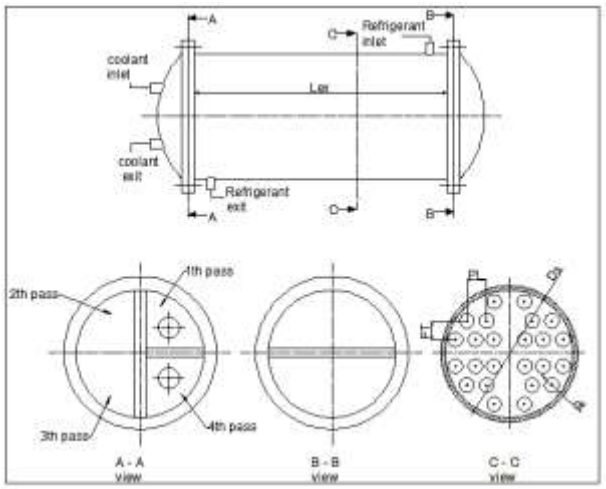

Figure 5. Layout of the tested condenser

The results of Emerson's method for the working conditions Case-1 through Case-3 are given in Table-4. Comparing the condenser area calculated from Emerson's method and the design code, the maximum absolute deviation is 7.6 %.

Table 4. Results of Emerson's method

	Case 1	Case 2	Case 3
A_T (m^2)	1.132574	1.188147	1.13615
L_{ex} (m)	0.5045062	0.5292642	0.5060993

Because the design code examines a series of exchangers from tube counts, there are many alternative exchangers that would satisfy the given duty, therefore either capital cost or running cost should be considered for a better selection. Capital cost involves minimisation

of the heat transfer surface area, while the running cost involves minimum pressure drops. Since the pressure drops in refrigerant condensers are usually small due to the lower flow rates, especially on refrigerant side, the design code considers the minimum heat transfer surface area for decreasing the initial cost. The code also provides several design parameters that can be useful for the designer, such as the heat transfer area and heat rates of the two-phase flow zone, and the refrigerant temperature ($T_{r,sh}$) where condensation just commences on the surface, heat transfer coefficients in each zone, etc. (see Table-5).

Table 5. Detailed results from the validation code

	Unit	Case-1	Case-2	Case-3
Q_{tot}	(W)	3,837.7	4,027. 5	3,972.9
Q_{sh}	(W)	3,51.8	332.0	271.6
Q_{tp}	(W)	3,379.7	3,613.8	3,660.9
Q_{sb}	(W)	106.1	81. 7	40.4
A_{tot}	(m^2)	1.0462	1.0426	1.0590
A_{sh}	(m^2)	0.4172	0.4174	0.4152
A_{tp}	(m^2)	0.5580	0.5763	0.6201
A_{sb}	(m^2)	0.0710	0.0489	0.0237
L_{ex}	(m)	0.7710	0.7680	0.7800
$T_{r,sh}$	(°C)	70.3	65.6	59.9
$T_{w,sh}$	(°C)	61.5	56.6	51.5
$T_{w,tp}$	(°C)	56. 6	51.3	46.2
$h_{r,sh}$	($W/m^2.K$)	62.5	58.2	52.8
$h_{r,tp}$	($W/m^2.K$)	2,020.4	2,089.9	2,228.9
$h_{r,sb}$	($W/m^2.K$)	368.3	369.5	365.9
U_{sh}	($W/m^2.K$)	60.3	56.2	51.3
U_{tp}	($W/m^2.K$)	778.4	788.5	807.5
U_{sb}	($W/m^2.K$)	302.1	302.3	299. 3
ΔP_s	(Pa)	2.8	3.3	3. 6
ΔP_t	(Pa)	26.5	26.6	26.7

CONCLUSION

A design code using the tube count table is presented for designing a horizontal shell and tube refrigerant condenser. The model of the design code is based on the three-zone approach for the refrigerant side, while the overall calculation approach is for the coolant side. In the present model, the wet wall de-superheating zone is factored into a condensation region and the constant wall temperature in each zone is assumed. The heat loss and the effect of pressure drop in the shell on the condensation temperature are neglected. The model is experimentally validated by a validation code derived from the design code. The results from the model are in good agreement with the experimental results. The maximum deviations between the output of the code and the measured values for the heat rate and heat transfer area are 13% and 7%, respectively. These are acceptable errors considering the uncertainty of the heat load, which is 11%. The results of the design program are in good agreement with the results from Emerson's method. Comparing the condenser area calculated from Emerson's method and the design program, the maximum absolute deviation is 7.6 %.

REFERENCES

Basu, R.S. and Wilson, D.P. (1989) Thermophysical properties of 1,1,1,2-tetrafluoroethane (R-134a). *International Journal of Thermophysics*, 10(3), 591-603.

Bell, K, J., & Ghaly,M.A.(1973). An approximate generalized design method for multicomponent partial condensers. *Heat transfer, AIChE Symposium Series*, 69(131), 72-79.

Brown, M.W. & Bansal, P.K. (1999). An overview of condensation heat transfer on horizontal tube bundles. *Applied Thermal Engineering*, 19, 565-594.

Burlingame, R.S. (1984). Mean temperature difference for shell and tube heat exchangers with condensing on the shell side. *Heat Transfer Engineering*, 5(3), 34-47.

Butterworth, D. (Ed.) (1983). Condensers: Theory and practice. *The Institution of Chemical Engineers Symposium Series*, no 75. New York : Pergamon Press.

Cleland, A.C. (1994). Polynomial curve-fits for refrigerant thermodynamic properties: extension to include R-134a. *International Journal of Refrigeration*, 17(4), 245-249.

Ferrari, G., Mischiatti, M., Naviglio, A., & Rocca, S. (1986). Advances in the design and analysis methods of shell and tube heat exchangers with condensation shell side. In Tien C.L., Carey V.P., Ferrell, J.K., (Eds.), *Heat transfer, Proceedings of The Eighth International Heat Transfer Conference* (pp. 2697-2702). San Francisco: Hemisphere Publishing Corp.

Grant, I.D.R. & Chisholm, D. (1979). Two-phase flow on the shell-side of a segmentally baffled shell-and-tube heat exchanger. *Transactions of the ASME*, 101, 38-42.

Hewitt, G.F., Shires, G.L. and Bott, T.R. (1994). *Process Heat Transfer.* New York: CRC Press, (Ch. 18).

Holman, J.P. (1994). Experimental methods for engineers, (6th ed.). New York: McGraw-Hill Inc. (Ch. 3).

Incropera, F.P., & Dewitt, D.P. (2007). *Fundamentals of heat and mass transfer*. USA: John Wiley &Sons, (Ch. 9).
Kakaç S. & Liu H. (1998). Heat exchangers, selection, rating, and thermal design. New York: CRC press, (Ch. 3).

Karlsson,T., & Vamlin, L. (2005). Flow fields in shell-and-tube condensers: comparison of a pure refrigerant

and a binary mixture, *International Journal of Refrigeration*, 28, 706–713.

Llopis, R., Cabelloa, R., & Torrellab, E. (2008). A dynamic model of a shell-and-tube condenser operating in a vapour compression refrigeration plant. *International Journal of Thermal Sciences* 47 926–934.

Marto, P.J. (1984). Heat transfer and two-phase flow during shell-side condensation. *Heat Transfer Engineering*, 5(1-2), 31-61.

Mohanty, A.K. (1988). Numerical design of a shell-and-tube steam condenser. In Shah, R.K., Subbarao, E. C., & Mashelkar, R. A. (Eds.), *Heat transfer equipment design*, (pp.559-570). New York: Hemisphere Publishing Co.

Mueller, A.C. (2002). Mean Temperature Difference. In Hewitt G.F. (Ed.), *Heat Exchanger Design Handbook* (Section 3.4.8), New York: Begell House, Inc.

Paul, H. (1986). An application of stochastic geometric condemning to heat exchanger design. *Computers & Industrial Engineering*, 10(3), 253-262.

Rubin F.L. (1981). Multi-zone condensers: de-superheating, condensing, sub-cooling. *Heat Transfer Engineering*, 5(1), 49-59.

APPENDIX A

Emerson Method

1. Plot the temperature versus specific enthalpy for the shell side stream

2. Guess a value $T_{r,eff}$ (between $T_{r,in}$ and $T_{r,out}$)

3. Calculate $\overline{T}_c$ as follows,

$$\overline{T}_c = T_{r,eff} - \frac{T_{c,out} - T_{c,in}}{\ln\left[\left(T_{r,eff} - T_{c,in}\right) \Big/ \left(T_{r,eff} - T_{c,out}\right)\right]}$$

4. Calculate θ_m as follows,

$$\frac{1}{\theta_m} = \frac{1}{i_{r,in} - i_{r,out}} \sum_J \frac{\left(\Delta i_r\right)_J}{\left(\theta_{ln}\right)_J}$$

5. Recalculate $T_{r,eff}$ from the equation below,

$$T_{r,eff} = \theta_m + \overline{T}_c$$

6. Repeat the calculation from step 3 until convergence is obtained.

7. Plot $\overline{T}_c$ as a horizontal line on the operating diagram

8. Divide the diagram into zones (Figure-A1) and calculate required area for each zone then calculate the total exchanger as follows;

$$A_J = \frac{\dot{m}_r \left(\Delta i_r\right)_J}{U_J \left(\theta_{ln}\right)_j}$$

$$A_{tot} = \sum_J A_J$$

$$\left(\theta_{ln}\right)_J = \frac{\left(T_{r,in} - \overline{T}_c\right)_J - \left(T_{r,out} - \overline{T}_c\right)_J}{\ln \dfrac{\left(T_{r,in} - \overline{T}_c\right)_J}{\left(T_{r,out} - \overline{T}_c\right)_J}}$$

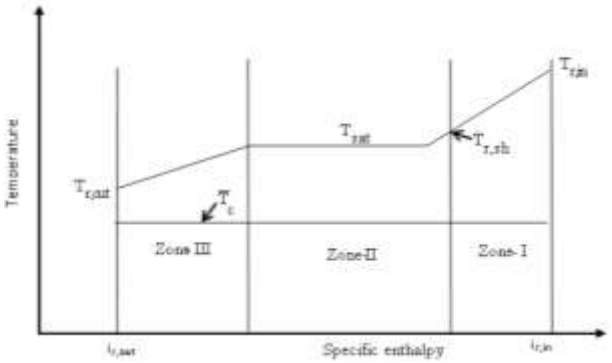

Figure A1. Exchanger Operating Diagram

Yusuf Ali Kara is an Associate Professor in the Department of Mechanical Engineering, University of Ataturk, Turkey. He received his Ph.D. in 1999 from Ataturk University. His main research interests are heat pumps, heat exchangers, and renewable energy. He has published seven articles in international journals.